

Highly sensitive TiO₂ based photodetector for environmental sensing applications

S.H. Mohamed^{1,2}, Mohamed Rabia³, M. A. Awad², Mohamed Asran Hassan²

¹Faculty of Graduate Studies and Environmental Research, Sohag University, 82524 Sohag, Egypt

²Physics Department, Faculty of Science, Sohag University, 82524 Sohag, Egypt

³Nanomaterials Science Research Laboratory, Chemistry Department, Faculty of Science, Beni-Suef University, Beni-Suef, 62514, Egypt.

Received: 2 Jan. 2025, Revised: 17 Jan. 2025, Accepted: 31 Jan. 2025 Published online: 1 Apr. 2025

Abstract: TiO₂ thin films were fabricated using reactive direct current magnetron sputtering for the possible utilization as visible and/or IR-light photodetectors. The structure, chemical composition, morphology, optical and I-V characteristics were examined. X-ray diffraction inferred the existence of body centered tetragonal anatase crystallographic phase oriented around (101) plain. The chemical compositional analysis via EDAX indicated TiO_{2.1} stoichiometry. Nanoparticle morphology that is uniformly distributed were observed by SEM investigations. High transmittance over the visible and near spectral ranges with optical band gap of 3.29 eV were observed for the TiO₂ thin films. The generated light current values at 1 V bias voltage were 0.251, 0.160 and 0.149 $\mu\text{A}/\text{cm}^2$ for illumination with light of 440, 540 and 730 nm, respectively. The reported TiO₂ based photodetector has good sensitivity comparable with the previously published works which infers that it may be used in environmental sensing applications.

Keywords: TiO₂ thin films; structural properties; morphology; optical characteristics; photodetector

1. Introduction

Now a days monitoring the environment requires a broad-range of photodetectors from the ultraviolet (UV) to the infrared (IR) [1,2]. For example, detection of pollution mainly depends on UV spectroscopy, where the detectors measure the absorption lines strength for these pollutants such as ozone, nitrous oxides, and sulfur dioxide. Fluorescence spectroscopy capable of detecting very small amounts of pollutants such as sulfur oxides, benzene, xylene and toluene, which can be measured at a parts-per-billion level [3]. To monitor solid particulates in water and air, more straightforward techniques are utilized. In this case, the quantity of scattered light via the particles gives a measure for levels of pollution. In many cases ample light is available, so photodetectors may be utilized, taking advantage of their fast response times and robustness [4].

As a semiconductor titanium dioxide (TiO₂) is characterized by a wide band gap (> 3.0 eV), low cost, high stability and photo-active properties. Therefore, it has received a significant interest and it has found numerous applications in various fields such as solar cells [5], energy storage [6], photocatalytic, antioxidant and antibacterial applications [7,8], photodetectors [9], etc.

In the field of photodetectors TiO₂ based photodetectors have common view over photodetectors

including better control, good sensing properties, enhanced catalytic activity, self-sufficiency, better communication proficiencies, response speed and high sensitivity with low cost user-friendly [10]. Therefore, TiO₂ based photodetectors have become an important semiconductor device because of their applicability in different day-to-day life appliances like environmental monitoring, compact smoke detectors, optical communication, imaging, remote control, chemical analysis and disk players [10-14]. However, there is remaining a challenging task which is the fabrication of a very thin TiO₂ based photodetector device [15]. Therefore, in this work the TiO₂ thin films with thickness of 230 nm were prepared using direct current (dc) reactive magnetron sputtering as visible and/or IR-light photodetectors. Moreover, the crystal structure, morphology and optical characteristic of the films were investigated.

2. Experimental

TiO₂ thin films were deposited using dc reactive magnetron sputtering from metallic Ti target. The preparation was achieved on FTO, glass and Si (100) substrates which were previously heated to 200°C. Deposition was started after reaching a base pressure of 3.1×10^{-7} mbar. Ar and O₂ of 75 and 25 sccm, respectively, were used for the deposition of the films. The deposition was achieved at constant power of 100 W. The working

pressure was 1.2×10^{-2} mbar. The film thickness was fixed to 230 nm by controlling the deposition time.

ZEISS scanning electron microscope (SEM) was used to examine the surface morphology. The chemical composition of the films was estimated from the energy dispersive analysis of X-ray (EDAX) unit which is attached to the SEM. The crystallographic identification was achieved using X-ray diffraction (XRD) model Bruker D8 ADVANCE diffractometer. The PEAK UV-Vis-NIR spectrophotometer (model C-7200) was utilized to measure transmittance (T) and the reflectance (R) of the films.

The characteristics of the TiO₂ photodetector on FTO substrates were conducted on CHI660E electrochemical workstation. The I-V measurements were carried out in the voltage range from -1 to +1 V. 100 mW/cm² xenon lamp was utilized as simulated light source, in which glass/FTO/TiO₂ presents the photoelectrode. Silver paste was used to make the electrodes on two sides of the photodetector. The effect of monochromatic light wavelength on the performance the deposited photodetector was investigated with 440, 540 and 730 nm wavelengths. The light reproducibility was assessed via on/off chopped current measurements with time. The measurements were done at atmospheric conditions and at room temperature.

3. Results and discussions

3.1 EDAX, XRD, SEM and optical examinations

Fig. 1 shows EDAX spectrum of sputtered film on Si (100) substrate. Oxygen and titanium peaks are existing together with silicon and small carbon peaks. The silicon peak comes from the Si (100) substrate and the carbon peak comes from the contamination of the film's surface by the hydrocarbons after sputtering or during the EDAX measurement. The estimated Ti and O atomic percentage ratios are 31.76 at.% and 68.24 at.%, respectively. Thus, the obtained stoichiometry is TiO_{2.1}. The excess oxygen in the film may be physically trapped, chemically bonded and/or adsorbed on the surface [16].

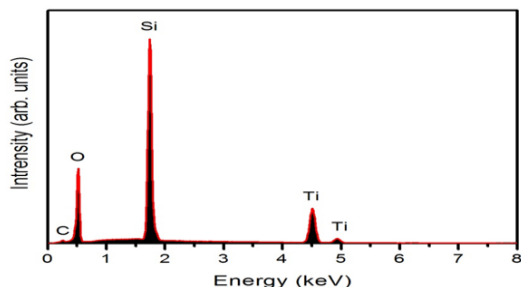


Fig. 1: Typical EDAX spectra of TiO₂ thin film deposited on Si (100) substrate.

Fig. 2 displays the XRD pattern of the sputtered TiO₂ thin film on glass substrate. The pattern of pure TiO₂ displays several crystalline peaks which are indexed to body

centered tetragonal anatase crystallographic phase (COD: 01-089-4921). The phase is highly oriented around (101) plane. The crystallite size (L) is calculated from the Scherrer equation using (101) peak.

$$L = \frac{K\lambda}{\beta \cos\theta} \quad (1)$$

where λ (nm) is the wavelength of the XRD radiation, β is the full width at half maximum of peaks (101) in radian located and K is the shape factor which is usually taken as about 1. The obtained L value is found to be 18.3 nm.

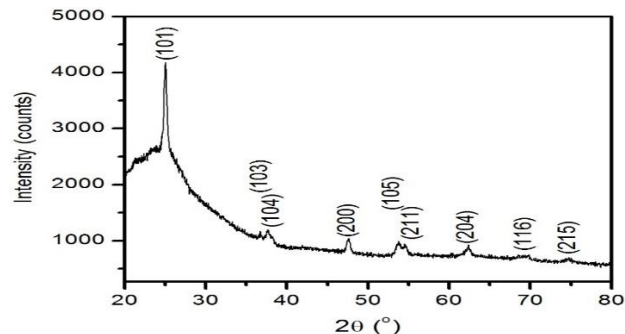


Fig. 2: XRD pattern of TiO₂ thin film deposited on glass substrate.

Fig. 3 presents the surface morphology of the TiO₂ film displayed from SEM. The film exhibits quite homogeneous and uniform nanoparticles morphology. The diameters of nanoparticles are in the range 10–36 nm. Besides to nanoparticles there are small pinholes-like nanodefects. Similar morphology was reported previously for titanium oxynitride films prepared by dc reactive magnetron sputtering [18].

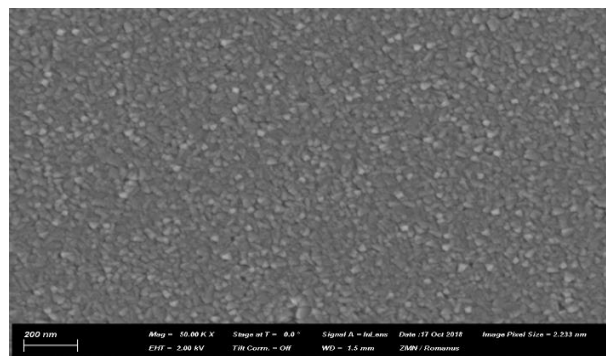


Fig. 3: SEM image of TiO₂ thin film deposited on Si (100) substrate.

The optical reflectance and transmittance of TiO₂ film on glass substrate as functions of wavelength are presented in Fig. 4. The transmittance of TiO₂ is high over the entire visible and near infrared ranges. Some interference fringes are observed in both transmittance and reflectance due to the difference in refractive index between TiO₂ and air, and TiO₂ and glass. The existence of the interference fringes infers the good quality of the films.

The absorption coefficient (α) of TiO₂ film is calculated from the reflectance and transmittance spectra and thickness (d) of the film via the equation:

$$\alpha = \frac{1}{d} \ln \left(\frac{1-R}{T} \right) \quad (2)$$

The optical band gap (E_g) is obtained by proposing allowed indirect transition from Tauc's formula:

$$(\alpha h\nu)^{\frac{1}{2}} = A(h\nu - E_g) \quad (3)$$

where ν is to the frequency of the incident light and A is a constant. Fig. 4b presents the $(\alpha h\nu)^{\frac{1}{2}}$ versus $h\nu$ plot with the linear fit to a straight line. The E_g value is obtained through the extrapolation of the linear part to intercept with $h\nu$ axis. The obtained E_g value is 3.29 eV which is very near to the value 3.2 of bulk anatase [19]. However, it is lower than the values 3.32-374 eV of TiO₂ prepared by reactive dc magnetron sputtering at various working pressures [20].

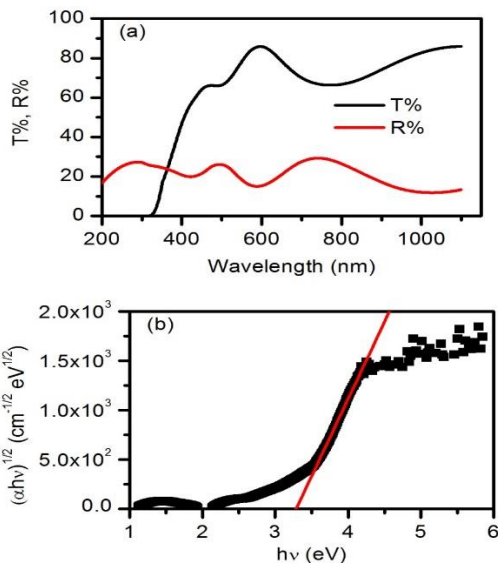


Fig. 4: Optical reflectance and transmittance as a function of wavelength (a), and $(\alpha h\nu)^{\frac{1}{2}}$ versus $h\nu$ plot (b) for TiO₂ thin film deposited on glass substrate.

3.2 The Photodetector Electrochemical characterization

The response of the deposited FTO/TiO₂ photodetector at different wavelengths of 440, 540 and 730 nm is presented in Fig. 5. Both the dark current (I_{Dr}) and light current (I_{Ph}) increase with bias potential. This is agreement with the reported results for TiO₂ photoelectrodes [21]. It is observed that the generated dark current density (I_o) at +1 V has a very low value of 0.046 $\mu\text{A}/\text{cm}^2$, concerned to the original charges of FTO/TiO₂ semiconductor. The generated I_{ph} values at 1 V bias voltage are 0.251, 0.160 and 0.149 $\mu\text{A}/\text{cm}^2$ for illuminated light with 440, 540 and 730 nm, respectively. It is observed that the photodetector

responded strongly to the different light wavelengths. During light irradiation electron and hole pairs are photo-produced. Thus, the decrease in I_{Ph} values with increasing wavelength is attributed to the disparity in the capability of the incident photons to generate charge carriers. This infers that the photodetector is capable to respond to various light regions with various sensitivities. The FTO/TiO₂ photodetector has the highest sensitivity in the visible region.

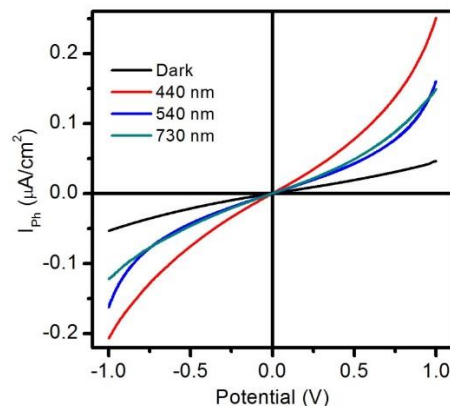


Fig. 5: The response of the deposited FTO/TiO₂ photodetector at different wavelengths.

Fig. 6 displays multiple photo-switching cycles at a bias potential of 1 V. It is observed that the elevation time is almost the same as the decay time. This infers that photogenerated carriers in FTO/TiO₂ photodetector are fast in both generation and recombination which confirms the fast charge transport rate. The response speed is a substantial property for the photodetector, which indicates how fast the high- and low-current states can be changed. The response times (fall and rise times) are set as times needed for the current to increase from 10% to 90% or decrease from 90% to 10% of the highest value after on/off cycling. The time of response is almost 6 s. Table 1 shows a comparison between the sum of the devices previously published and the TiO₂ based photodetector reported in this work. The FTO/TiO₂, presented in this work, exhibits higher sensitivity (I_{Ph}/I_{Dr}) compared with other photodetectors.

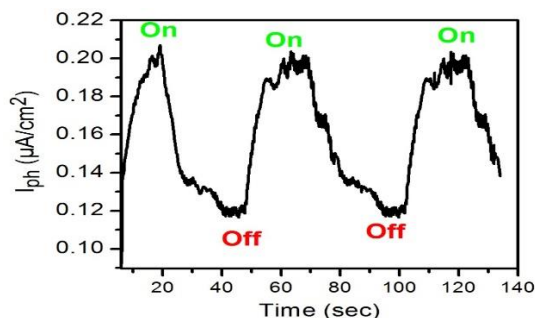


Fig. 6: displays multiple photo-switching cycles at a bias potential of 1 V for FTO/TiO₂ photodetector.

Table 1: Comparison between the present FTO/TiO₂ photodetectors and some of the photodetectors published previously.

Material	λ (nm)	Bias (V)	I_{ph}/I_{Dr}	Ref.
Pt/TiO ₂ /P-Si (111)/In	405	5	2.32	[22]
TiO ₂ /water solid-liquid	365	0	200	[23]
Al/CuO/Al	808	5	4.05	[24]
FTO/TiO ₂ /TNA/water solid-liquid	365	0	200	[25]
Cu/CuO/Ag	UV source	0.01	~69	[26]
In ₂ O ₃ /CuO	589	5	2.6	[27]
CuO	250-900	20	1.25-1.8	[28]
FTO/TiO ₂	440	1	5.39	This work

4. Conclusion

TiO₂ thin films were deposited on onto glass, Si (100) and FTO substrates. XRD, SEM and EDAX analysis revealed single body centered tetragonal anatase crystallographic with nanoparticle morphology and TiO_{2.1} stoichiometry that contained excess oxygen. The films have high transmittance over the visible and near infrared spectral ranges. The E_g value was 3.29 eV. The I_{ph} values at 1 V bias voltage were 0.251, 0.160 and 0.149 $\mu\text{A}/\text{cm}^2$ when irradiated with light of 440, 540 and 730 nm wavelength, respectively. The FTO/TiO₂ photodetector has good sensitivity and it may be used in environmental sensing applications.

Conflicts of interests

The authors declare that that present work does not have conflict of interest.

Author Contribution

Material preparation, data collection and analysis were performed by S.H. Mohamed, Mohamed Rabia, M. A. Awad and Mohamed Asran Hassan. The first draft of the manuscript was written by S.H. Mohamed and all authors commented on previous versions of the manuscript. All authors read and approved the final manuscript.

Research Data Policy and Data Availability Statements

The data are available on reasonable request from the corresponding author.

5. References

[1] N. Jain, D. Kumar, K. Bhardwaj, R. K. Sharma, J. Holovsky, M. Mishra, Y. K. Mishra and S. K. Sharma, "Heterostructured core-shell metal oxide-based nanobrushes for ultrafast UV photodetectors", *Mater. Sci. Eng. R*, vol.

160, pp. 100826, 2024.

[2] A. B. U. Rahman, S. Begum, N. M. S. Kaawash, M. Y.H. Thabit, D. I. Halge, P. M. Khanzode, S. J. Shaikh, V. N. Narwade, P. S. Alegaonkar and K. A. Bogle, "p-NiO/n-ZnO heterojunctions for visible-blind UV and IR photodetectors: A low-temperature fabrication approach", *Physica B: Cond. Matter.*, vol. 694, pp. 416478, 2024.

[3] M. Ródenas, T. Vera, A. Muñoz and F. Villanueva, "Advantages and limitations of the analytical methods currently employed for the assessment of inorganic pollutants in indoor and outdoor air", *TrAC- Trends Anal. Chem.*, vol. 181, pp. 118034, 2024.

[4] Y. Yuan, H. Tao, H. Wang, J. Liu, Y. Zhang, Q. Fu, H. Zhao, T. Di, H. Long and S. Yao, "The effect of UVO treatment on TiO₂-MAPbI₃ heterostructure photodetector prepared in air atmosphere", *Mater. Sci. Semicond. Process.*, vol. 172, pp. 108079, 2024.

[5] S. Mathur, V. Bishop, A. Swindle and W. Wei, "Enhanced performance of Bi₂S₃/TiO₂ heterostructure composite films for solar cell applications", *J. Photochem. Photobiol.*, vol. 25, pp. 100256, 2025.

[6] M. Z. Ullah Shah, J. Feng, F. BiBi, M. Sajjad, M. T. Qureshi, A. Shah, M. S. Shah, A. M. Khaled and M. S. Salem, "Enhanced energy storage with TiO₂/NiO/ZnO core-shell heterostructures in hybrid battery-supercapacitor applications", *J. Alloys Compod.*, vol. 1013, pp. 178548, 2025.

[7] N. Thakur, N. Thakur, A. Kumar, V.K. Thakur, S. Kalia, V. Arya, A. Kumar, S. Kumar and G. Z. Kyzas, "A critical review on the recent trends of photocatalytic, antibacterial, antioxidant and nanohybrid applications of anatase and rutile TiO₂ nanoparticles", *Sci. Total Environ.*, vol. 914, pp. 169815, 2024.

[8] S. Hassaballa, A Aljabri, S. H. Mohamed, N. M. A. Hadia and M. A. Awad, "Synthesis, structural, photocatalytic, wettability and optical properties of TiO₂ films on polymethyl methacrylate substrates", *Phys. Scr.*, vol. 98, pp. 055801, 2023.

[9] S. Izmirlı and S. Cavdar, "Effect of film thickness on photodiode and photodetector performance of Titanium dioxide (TiO₂) prepared via solution Assisted spin coating method", *Appl. Surf. Sci.*, vol. 688, pp. 162187, 2025.

[10] C. Ghosh, A. Dey, I. Biswas, R. K. Gupta, V. S. Yadav, A. Yadav, N. Yadav, H. Zheng, M. Henini and A. Mondal, "CuO-TiO₂ based self-powered broad band photodetector", *Nano Mater. Sci.*, vol 6, pp. 345-354, 2024.

[11] M. Zhou, S. Zhang and Y. Wang, "ZnS-shelled and Zn-doped CuInS₂ quantum dots for TiO₂-based UV photodetectors", *Chem. Phys. Lett.*, vol. 862, pp. 141861, 2025.

- [12] S. Lee, M. Kim, B. J. Ahn and Y. Jang, "Odorant-responsive biological receptors and electronic noses for volatile organic compounds with aldehyde for human health and diseases: a perspective review", *J. Hazard. Mater.*, vol. 455, pp.131555, 2023.
- [13] Y. Shehu, S. A. M. Samsuri, Naser M. Ahmed, S. Aslam, "Fabrication of TiO₂ nanoparticles/porous-silicon heterostructure photodetector for UV detection", *Optik*, vol 304, pp. 171784, 2024.
- [14] J. Chen, J. Xu, L. Kong, S. Shi, J. Xu, S. Gao, X. Zhang and L. Li, "Self-powered SnS_x/TiO₂ photodetectors (PDs) with dual-band binary response and the applications in imaging and light-encrypted logic gates", *J. Colloid Interface Sci.* vol. 663, pp. 336-344, 2024.
- [15] Y. Wang, A. J. Muhowski, L. Nordin, S. Dev, M. Allen, J. Allen and D. Wasserman, "High-speed long-wave infrared ultra-thin photodetectors", *APL Photonics* vol. 9, pp.016117, 2024.
- [16] S.H. Mohamed, O. Kappertza, J.M. Ngaruiya, T.P. Leervad Pedersen, R. Drese and M. Wuttig, "Correlation between structure, stress and optical properties in direct current sputtered molybdenum oxide films", *Thin Solid Films*, vol. 429, pp. 135-143, 2023.
- [17] B. D. Cullity, "Elements of X-Ray Diffraction", 2nd ed. AddisonWesley, Reading, MA, pp.102, 1979.
- [18] A. M. Abd El-Rahman and S. H. Mohamed, "Preparation and characterization of nanostructured titanium oxynitride films for the application in self-cleaning and photoelectrochemical water splitting", *Thin Solid Films*, vol. 698, pp. 137864, 2020.
- [19] L. Chiodo, J.M. Garcia-Lastra, A. Iacomino, S. Ossicini, J. Zhao, H. Petek and A. Rubio, "Self-energy and excitonic effects in the electronic and optical properties of TiO₂ crystalline phases", *Phys. Rev. B: Condens. Matter.*, vol. 82, pp. 045207, 2010.
- [20] F. A. Hernández-Rodríguez, R. Garza-Hernández, M. R. Alfaro-Cruz and L. M. Torres-Martínez, "Tunable structure of TiO₂ deposited by DC magnetron sputtering to adsorb Cr (VI) and Fe (III) from water", *Heliyon* vol. 10, pp. e27359, 2024.
- [21] Z. Li, Z. Li, C. Zuo and X. Fang, "Application of Nanostructured TiO₂ in UV Photodetectors: A Review", *Adv. Mater.*, vol. 34, pp. 2109083, 2022.
- [22] A. M. Selman, Z. Hassan, M. Husham and N. M. Ahmed, "A high-sensitivity, fast-response, rapid-recovery p-n heterojunction photodiode based on rutile TiO₂ nanorod array on p-Si (111)", *Appl. Surf. Sci.*, vol. 305, pp. 445-452, 2014.
- [23] W.J. Lee and M. H. Hon, "An ultraviolet photo-detector based on TiO₂/water solid-liquid heterojunction", *Appl. Phys. Lett.* 99 (2011) 251102.
- [24] K.M. Chahrouh, N.M. Ahmed, M. Hashim, N.G. Elfadill, M. Bououdina, "Self-assembly of aligned CuO nanorod arrays using nanoporous anodic alumina template by electrodeposition on Si substrate for IR photodetectors", *Sens. Actuat. A: Phys.*, Vol. 239, pp. 209-219, 2016.
- [25] Y. Xie, L. Wei, G. Wei, Q. Li, D. Wang, Y. Chen, S. Yan, G. Liu, L. Mei and J. Jiao, "A self-powered UV photodetector based on TiO₂ nanorod arrays", *Nanoscale Res. Lett.*, vol. 8, pp. 188, 2013.
- [26] A.M. Anand, A. Raj, J.A. Salam, R.A. Nath and R. Jayakrishnan, "Photoconductivity in self-assembled CuO thin films", *Mater. Renew. Sustain. Energy*, vol. 13, pp. 45-58, 2024.
- [27] A. M. Abd El-Rahman, S. H. Mohamed, A. Ibrahim, A. A. Alhazime, M. A. Awad, "Optoelectronic characteristics of In₂O₃/CuO thin films for enhanced vis-light photodetector", *J. Mater. Sci.: Mater. Electron.*, vol. 35, pp. 1910, 2024.
- [28] A. Tripathi, T. Dixit, J. Agrawal and V. Singh, "Bandgap engineering in CuO nanostructures: Dual-band, broadband, and UV-C photodetectors", *Appl. Phys. Lett.*, vol. 116, pp. 111102, 2020.